IEEE Access
Multidisciplinary | Rapid Review | Open Access Journal

Received January 3, 2019, accepted January 22, 2019, date of publication January 31, 2019, date of current version February 14, 2019.

Digital Object Identifier 10.1109/ACCESS.2019.2895502

The Sensitivity Design of Piezoresistive Acceleration Sensor in Industrial IoT

CHEN DONG[1,2,3], (Member, IEEE), YIN YE[1,2], XIMENG LIU[1,2], (Member, IEEE), YANG YANG[1,2], (Member, IEEE), AND WENZHONG GUO[1,3], (Member, IEEE)

[1]College of Mathematics and Computer Science, Fuzhou University, Fuzhou 350116, China
[2]Fujian Provincial Key Laboratory of Information Security of Network Systems, Fuzhou University, Fuzhou 350116, China
[3]Fujian Provincial Key Laboratory of Network Computing and Intelligent Information Processing, Fuzhou University, Fuzhou 350116, China

Corresponding author: Wenzhong Guo (fzugwz@163.com)

This work was supported in part by the National Natural Science Foundation of China under Grant 61672159, Grant 61872091, Grant U18042631, and Grant 61702105, in part by the Science Foundation of the Fujian Province, China, under Grant 2018J01793, and in part by the Foundation of the Education Department of Fujian Province, China, under Grant JAT170099.

ABSTRACT Piezoresistive acceleration sensors are widely used in various fields of the industrial Internet of Things because of their lightweight, fast response, and small size. The structural sensitivity of the sensor affects the accuracy of the measurement. And the sensitivity that the traditional method designs are only a feasible solution, not an optimal solution. Due to the differences in factory processes, the optimization of structural sensitivity is an NP-hard problem. To solve the design problem of structural sensitivity, we adopt the swarm intelligence algorithm in this paper, and we design a model for the structural sensitivity of the piezoresistive acceleration sensor. In addition, an improved grasshopper optimization algorithm (CC-GOA) that combines chaos strategy and Cauchy mutation is proposed to optimize the structural sensitivity of the piezoresistive acceleration sensor, and the structure of the sensor is composed of four beams and mass block. The experiments are compared with six well-known algorithms on 16 benchmark functions to verify the algorithm performance of CC-GOA, and then, the structural sensitivity of the piezoresistive acceleration sensor is optimized by CC-GOA. The results indicate that the piezoresistive acceleration sensor is designed with high sensitivity and superiority.

INDEX TERMS Industrial Internet of Things, piezoresistive acceleration sensor, structural sensitivity optimization, grasshopper optimization algorithm.

I. INTRODUCTION

Internet of Things is information sensing devices such as radio frequency identification (RFID) [1], the global positioning system (GPS) [2], sensors and so on, which connects any item with the Internet according to the agreed protocol, exchanges information and communicates to realize intelligent identification and positioning [3], management and monitoring [4]. Its purpose is to realize the connection between objects and objects, people and objects, all items and networks, so as to facilitate identification, management and control. Internet of things has the characteristics of comprehensive perception [5], reliable transmission [6], intelligent control [7], data fusion [8] and has been widely applied in all walks of life. For example, intelligent logistics [9] optimizes the distribution route and service efficiency, and realizes the transparency, integration and intelligence of the logistics and distribution system applications; intelligent transportation [10] is applied for issuing weather warnings and speed limit adjustment, metering routes to reduce vehicle congestion and emissions; smart building [11] requires video surveillance, access management, and environmental monitoring; industrial Internet of Things [12] gathers information readings from the field and delivers the data to the Internet for measurement and inspection in industry.

With the rapid development of the Internet of Things in many fields, a wide variety of sensors are also constantly upgrading, such as image sensor, pressure sensor, gas sensor, and so on. Sensors are important components in the perception layer of the Internet of things, sensors are the means for the Internet of things to obtain information. Especially in the industrial sector, there are numerous types of sensors

The associate editor coordinating the review of this manuscript and approving it for publication was Siddhartha Bhattacharyya.

deployed on industrial Internet of things. Each sensor is an information source, and the information content is captured by different types of sensors. For instance, the gravity sensor is used to analyze engine vibration for automotive electronics systems; when the phone changes posture, orientation sensor feels the change in center of gravity for switching screen; acceleration sensor measures acceleration and converts to usable output signal for safety airbag of automobile, antilock brake system (ABC), traction control system (TCS).

Microelectromechanical Systems (MEMS) is originated in America, Japan and Europe in the 1960s as an advanced manufacturing technology, it combines integrated circuit technology and micromachining technology to the machine and manufacture micron materials based on semiconductor processing technology. At present, tens of thousands of sensors are manufactured by MEMS, acceleration sensors are no exception. Most manufacturing materials are made of silicon. Silicon accelerometer has incomparable advantages in volume, weight, cost and accuracy than sensors of other materials; this paper also considering the design of material differences. The most mature and widely used silicon accelerometers are mainly capacitive acceleration sensors and piezoresistive acceleration sensors.

In this paper, we mainly study piezoresistive acceleration sensor in the industrial Internet of Things. Most piezoresistive acceleration sensors use MEMS structures, that is, the core components of the entire sensor (mass block and cantilever beam) are etched from a single crystal silicon. Among them, piezoresistive acceleration sensors of cantilever beam are our research object, it has features of light weight, fast response, small size and used in various fields of the industrial Internet of Things, but the structural sensitivity is low. The sensitivity of piezoresistive acceleration sensor has a great impact on measurement results. If the sensitivity of sensors is too low, the acceleration measured with a large error. The error maybe cause serious safety incidents. According to the above statement, the structural sensitivity of piezoresistive acceleration sensor is crucial and has great research value.

Our main contributions can be summarized as follows:

- We propose the structural sensitivity design model of piezoresistive acceleration sensor based on the cantilever beam. The structure of piezoresistive acceleration sensor is composed of four beams and mass block. Taking into account the constraint of natural frequency, the length width, thickness of the cantilever beam, the objective function is to design the maximum of sensitivity.
- We propose an improved grasshopper optimization algorithm (CC-GOA) that combines chaos strategy and Cauchy mutation to optimize the structural sensitivity of piezoresistive acceleration sensor. Why not use other algorithms? We analyze the feasibility of the chaos strategy and Cauchy mutation in the improvement section, and conduct lots of experiments compared with six well-known algorithms on sixteen benchmark functions. We dissect the experimental data to verify the algorithm performance of CC-GOA. The results show CC-GOA have fast convergence rate and high convergence accuracy.
- We optimize the design for the structural sensitivity of piezoresistive acceleration sensor by GOA and CC-GOA. The results reveal the structural sensitivity of piezoresistive acceleration sensor is designed with high precision and superiority.

The rest of paper is organized as follows. Section II introduces the related work. In Section III, the brief overview of the piezoresistive acceleration sensor and original GOA are introduced. Section IV shows the mechanical structure of sensor and system architecture. Section V describes the mathematical model of the sensor and the modified CC-GOA in detail. The performance verification of algorithms is shown in Section VI. The optimization design of piezoresistive acceleration sensor in Section VII. Finally, Section VIII makes the conclusion.

II. RELATED WORK

There are many research literature about piezoresistive acceleration sensor. Vetrivel *et al.* [13] introduce the design and optimization of a doubly clamped acceleration sensor with integrated silicon nanowire piezoresistors. Messina *et al.* [14] elucidate an increment of the MMI is a viable optimization method for a single mass mechanical structure of a piezoresistive accelerometer sensor. Liu *et al.* [15] propose Timoshenko beams being modeled as double crossed clamped-clamped Timoshenko beams with a lumped moment of inertia at the free end and optimizes the eigenfrequency and sensitivity. Kazama *et al.* [16] propose novel high shock-resistant beam design for a piezoresistive three-axis accelerometer. Ghemari [17] propose an improvement of the piezoresistive accelerometer step and impulse responses by using appropriate parameters. Jakati *et al.* [18] propose a novel method based on the perforated diaphragm to increase the sensitivity of Piezoresistive Micro-Pressure sensor. Hari *et al.* [19] propose a novel nonplanar dual flexure geometry to achieve low cross-axis sensitivity. Defdaf *et al.* [20] reinforce the step and impulse responses of the piezoresistive accelerometer by damping rate and frequency range. Ghemari and Saad [21] propose a model relating the piezoresistive accelerometer displacement as a function of the measurement. enhance the trade-off between the sensitivity and the natural frequency of piezoresistive accelerometer. Wang *et al.* [22] improve the trade-off between the sensitivity and the natural frequency of piezoresistive accelerometer. Xu *et al.* [23] propose structure with SPBs for improving the tradeoff between the sensitivity and the resonant frequency of piezoresistive accelerometer.

As for the core algorithm, grasshopper Optimization Algorithm (GOA) [24] is introduced as a new and competitive population-based optimization algorithm by Australian scholars - Shahrzad *et al.* in 2017, which mimics the swarming behaviors of grasshopper insects in nature. GOA has aroused the interest of scholars and researchers. There are many engineering problems optimized by GOA.

Heidari *et al.* [25] propose a new hybrid stochastic training algorithm for multilayer perceptrons (MLPs) neural networks based on GOA. Rajput *et al.* [26] employ GOA to solve economic dispatch (ED) problem related to electrical power systems. Zhang *et al.* [27] propose a parameter-adaptive VMD method using GOA to analyze vibration signals from rotating machinery. Hamad *et al.* [28] use GOA for feature selection with SVM parameters optimization and automatic seizure detection in EEG signals. Amaireh *et al.* [29] combine ALO and GOA to minimize the maximum side lobe level (SLL). Mirjalili *et al.* [30] propose an archive and target selection mechanism based on GOA to solve multi-objective problems. Mafarja *et al.* [31] propose a search strategy using GOA to design a wrapper-based feature selection method. Arora and Anand [32] combine ten different chaotic maps to improve GOA on benchmark test functions. Potnuru and Tummala [33] apply GOA to improve the speed of BLDC motor drive. Mafarja *et al.* [34] use Chronological GOA for gene selection and cancer classification.

III. PRELIMINARIES

In this section, we introduce the piezoresistive acceleration sensor and a brief overview of original GOA.

A. PIEZORESISTIVE ACCELERATION SENSOR

The principle of the piezoresistive acceleration sensor is based on Newton's theorem and piezoresistive effect [35]. When the object moves with acceleration, the mass block is affected by an inertial force opposite to the acceleration direction, which deforms the cantilever beam. The deformation causes piezoresistive effect and the change of semiconductor resistance value on the cantilever beam results in the imbalance of the bridge path, so that the output voltage changes and the magnitude of the acceleration value can be obtained. And the level of structural sensitivity indicates the pros and cons of the design, the focus of this paper is to optimize the sensitivity of the piezoresistive acceleration sensor. There are many typical structures, such as single beam structure, double beam structure [36] and so on. This paper adopts four beams structure, that is, the entire sensor (mass block and four cantilever beams) are etched from single crystal silicon as Fig. 1.

B. ORIGINAL GOA

Original GOA mimics the swarming behaviors of grasshopper insects, and the solution of the problem is obtained by the comfort zone consisting of the attraction force and the repulsion force. The force is formed by the distance between individual grasshoppers. Firstly, a set of candidate solutions (each individual represents a grasshopper) are randomly generated to construct the initial artificial swarm. GOA considers a swarm N containing n grasshoppers ($N = 1, 2, \ldots, n$) in a D-dimensional continuous solution space. Each *i-th* grasshopper is represented by its position denoted as a D-dimensional vector: $X_i = (X_i^1, X_i^2, \ldots, X_i^d)$, where X_i^j is the *j-th* coordinate component of the position of the *i-th* grasshopper. The position of grasshopper X_i represents a possible solution to the optimization problem under study. The fitness value of grasshopper position can be obtained by evaluating the objective function at the grasshopper position. The fitness value is an indicator of the quality of the grasshopper position as a solution candidate to the optimization problem under study. In the comfort zone, the best position of the grasshopper (the target grasshopper) attracts the other grasshoppers, and the rest grasshoppers move towards the target grasshopper.

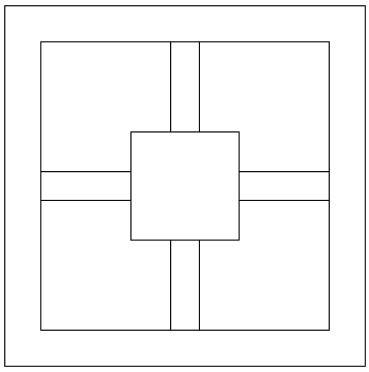

FIGURE 1. Four cantilever beams structure.

While s represents the strength of social forces function that defined as Eq. (1).

$$s(r) = fe^{\frac{-r}{l}} - e^{-r}. \tag{1}$$

where f is the intensity of attraction and l is the attractive length scale. The mathematical model is defined as Eq. (2).

$$X_i^d = c\Big(\sum_{j=1, j\neq i}^{N} c\frac{ub_d - lb_d}{2} s(|x_j^d - x_i^d|)\frac{x_j - x_i}{d_{ij}}\Big) + \widehat{T}_d. \tag{2}$$

where ub_d and lb_d represent respectively the upper bound and lower bound in the *D-th* dimension; d_{ij} is the distance between the *i-th* and the *j-th* grasshopper, which is calculated as $d_{ij} = |x_j\text{-}x_i|$; $\widehat{d}_{ij} = \frac{x_j - x_i}{d_{ij}}$ is a unit vector; T_d is the value of the best solution(the target grasshopper). Note that s is similar to Eq. (1). Here c is a decreasing coefficient to shrink the comfort zone as Eq. (3).

$$c = c_{max} - t\frac{c_{max} - c_{min}}{t_{max}}. \tag{3}$$

where c belongs to 0.00001 to 1, and c_{max} and c_{min} are respectively the maximum and minimum values of parameter c, $c_{max} = 1$, $c_{min} = 0.00001$; t indicates the current iteration, and t_{max} is the maximum number of iterations.

IV. PROBLEM FORMULATION

In this subsection, we know the mechanical structure of the sensor and introduce the system architecture.

A. THE MECHANICAL STRUCTURE OF THE SENSOR

When the spring is equivalent to the cantilever beam of the piezoresistive acceleration sensor, the elastic coefficient is k;

the gas damping is c; m is the mass of the mass block. The mechanical model of the piezoresistive acceleration sensor is shown in Fig. 2.

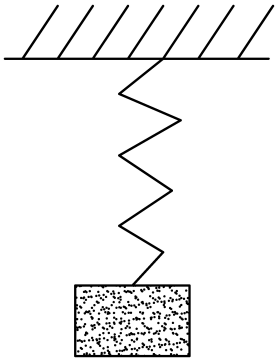

FIGURE 2. The mechanical model of piezoresistive acceleration sensor.

When the sensor is subjected to the acceleration a, the inertial force of the mass is calculated by $F = ma$. Therefore, the displacement produced by the mass block is as Eq. (4).

$$x = \frac{F_k}{k} = \frac{ma}{k}. \tag{4}$$

where the mass block generates a displacement x under the action of the stress F, which leads to the bending of the elastic beam. The elastic force F_k generated is opposite to the inertial force F and the system is in an equilibrium state, that is, $F_k = F$.

According to Newton's second law of motion, the force balance equation is as Eq. (5).

$$m\frac{d^2r}{dt^2} + c\frac{dr}{dt} + kr = ma. \tag{5}$$

where m is mass; r is displacement; c is damping factor and k is spring elasticity coefficient. d^2r/dt^2 represents the inertial force under acceleration; dr/dt is the damping force of the environment; kr represents the elastic force of the cantilever beam.

As for the deformation of the cantilever beam, the curvature equation of deformation deflection is as Eq. (6).

$$\frac{d^2w}{dx^2} = \frac{M}{EI}. \tag{6}$$

where the modulus of elasticity is E and the moment of inertia is I; the bending moment is M.

B. SYSTEM ARCHITECTURE

The system architecture is shown in Fig. 3, we aim to address the optimization design of piezoresistive acceleration sensor that consists of the cantilever beam and mass block. The computer can obtain related parameters information from the sensors, then set the constraint condition and range of variables based on the differences of factory processes, the data is processed by CC-GOA algorithm in the computer. CC-GOA calculates the relative optimal value of beam in different mass by the objective function. Our goal is to design the piezoresistive acceleration sensor with high sensitivity.

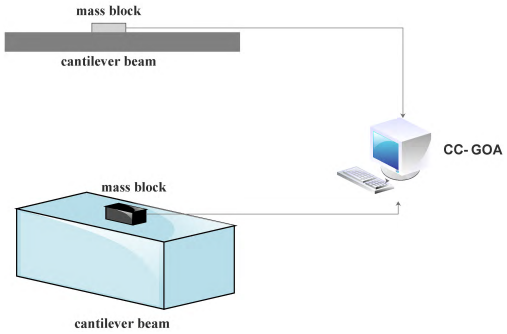

FIGURE 3. System architecture.

V. OPTIMIZATION GOAL AND METHOD

In this subsection, we analyze the force state of the sensor to infer optimization goal, then we propose the mathematical model for the piezoresistive acceleration sensor of four cantilever beams and mass block. In addition, we introduce the feasibility of chaos strategy and Cauchy mutation in CC-GOA.

A. THE FORCE STATE OF THE SENSOR

The stress generated at the root of the cantilever beam is as Eq. (7). The stress and the strain are converted by Eq. (8).

$$\sigma = \frac{6ml}{bh^2} * a. \tag{7}$$

$$\varepsilon = \frac{\sigma}{E} = \frac{6mla}{Ebh^2}. \tag{8}$$

where b is the width of the cantilever beam, h is the thickness of the cantilever beam, and l is the distance from the mass block to the root of the cantilever beam.

The strain that cantilever beam can bear is ε, the corresponding force P is as Eq. (9).

$$P = \varepsilon\frac{Ebh^2}{6l}. \tag{9}$$

The formula of inertia moment of rectangular section is $I = bh^3/12$. The displacement Y of the junction point is calculated by Eq. (10) between the support beam and the mass block along the y axis under the action of external force.

$$Y = -\frac{l^3}{12EI}P = -\frac{l^3P}{bh^3E}. \tag{10}$$

Due to the four beams structure, the force $P = ma/4$. So the structure sensitivity of the four beams is calculated by Eq. (11).

$$\eta = \frac{|Y|}{a} = \frac{ml^3}{4bh^3E}. \tag{11}$$

The four cantilever beams structure is regarded as a vibration system with four degrees of freedom, and its natural frequency is as Eq. (12).

$$f = \frac{1}{\pi}\sqrt{\frac{Ebh^3}{ml^3}}. \tag{12}$$

B. OPTIMIZATION GOAL

Taking into account the factory process, the frequency of the sensor is greater than 1000 Hz, the width of the beam is greater than 80 microns, the length of the beam is less than 800 microns, the thickness of beam greater than 30 microns, the mass of the mass block depends on the situation. The mathematical model of the design for the structure sensitivity is proposed as follow:

$$\begin{aligned}
&Consider\ \overrightarrow{X} = [b, l, h, m] = [x_1, x_2, x_3, x_4],\\
&Maximize\ \eta = \frac{x_2^3 x_4}{4 x_1 {x_3}^3 E},\\
&Subjectto\ h(x) = \frac{1}{\pi}\sqrt{\frac{E x_1 {x_3}^3}{{x_2}^3 x_4}} - 1000 > 0, \quad where\\
&\qquad x_1 \geq 80, \quad 0 < x_2 \leq 800,\ x_3 \geq 30,\\
&x_4\ depends\ on\ the\ situation.
\end{aligned}$$

The above mathematical model belongs to the constraint optimization problem. In general, the constrained problems are transformed into unconstrained problems, the penalty function method is mainly used as follow:

$$\begin{aligned}
&Minimize\ f(x)\\
&Subject\ to \begin{cases} g_i(x) \leq 0, & i = 1, 2 \ldots, g,\\ h_i(x) \geq 0, & i = 1, 2 \ldots, h,\\ m_i(x) = 0, & i = 1, 2 \ldots, m. \end{cases}\\
&Penalty\ function:\ F(x, M) = f(x) + M \sum_{i=1}^{m} |m_i(x)|\\
&\qquad + M \sum_{i=1}^{g} \max(g_i(x), 0)\\
&\qquad - M \sum_{i=1}^{h} \min(h_i(x), 0).
\end{aligned}$$

So the objective function constructed by the mathematical model is proposed as Eq.(13).

$$F(x, M) = \frac{1}{\eta} - M \sum_{i=1}^{4} \min\left(\frac{1}{\pi}\sqrt{\frac{E x_1 {x_3}^3}{{x_2}^3 x_4}} - 1000, 0\right). \quad (13)$$

where $F(x, M)$ is the penalty function; M is penalty factor.

C. THE PROPOSED CC-GOA

1) CHAOS INITIALIZES THE SWARM

Population initialization of evolutionary algorithms plays an important role in the final solution and convergence rate. In the original algorithm, random initialization is the most common method to initialize solution space. The solution initialized by the random method can not make certain that it is distributed over the entire solution space evenly. The random method may result in poor solution diversity and premature convergence problem. It is essential to ameliorate the approach of initializing the population. There are many research papers about chaos improves swarm intelligence algorithms, such as chaotic particle swarm optimization [37], chaotic artificial bee colony algorithm [38], chaotic whale optimization algorithm [39] and so on.

Chaotic motion [40] is a common phenomenon in nonlinear dynamic systems, which shows the behavior between random and rule. It has the characteristics: boundedness, randomness, regularity and ergodicity. The initial value of the standard GOA is randomly generated, and it is easy to gets stuck into local optimum. However, the chaotic sequence can iterate over all states in accordance with their own rules to conduct chaos optimization search in a certain range and search through the ergodic nature of chaos to jump out of local optimum. It is helpful to reinforce the efficiency and quality of the solution. In chaotic sequence, the chaotic value C_n at time n only depends on at time $n-1$. The most frequently-used chaotic equation is Logistic map, which is shown in Eq. (14) and Eq. (15).

$$C_n = \mu C_{n-1}(1 - C_{n-1}), \mu = 4, \quad (14)$$

$$X_i^j = X_{min}^j + C_n(X_{max}^j - X_{min}^j). \quad (15)$$

where μ is the control parameter of chaos. When μ is determined, any initial value $C_0 \in [0, 1]$. Obtaining a set of deterministic sequences: $C_1, C_2, \ldots, C_n$. When μ is equal to 4, the sequence is in a state of chaos completely. X_{min}^j and X_{max}^j are lower and upper bounds of position.

When the maximum iteration is 150 times, the individual distribution map of Logistic Chaos is as follows:

From Fig. 4 we know, The initial individual of Logistic chaos is distributed evenly in the solution space. The solution is generated between 0 and 1 with regularity and ergodicity. It causes rich population diversity and expedites the convergence speed of the algorithm.

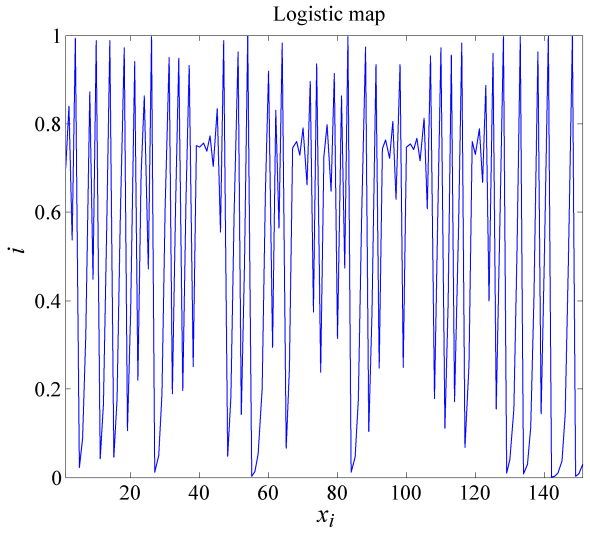

FIGURE 4. The Logistic map.

2) CAUCHY MUTATION PERTURBATION

The perturbation of the intelligent algorithm affects the quality of the final solution. When the algorithm converges into

local optimum, the perturbation of the position can help algorithm get out of local optimum and algorithm maybe find the more accurate solution in other position. Cauchy mutation is introduced to disturb the position in this paper. Cauchy distribution has a smaller peak at the origin and a longer peak at both ends. Therefore, Cauchy mutation can generate larger disturbance near the current mutation individuals and make the range of Cauchy mutation relatively wide. Cauchy mutation has been applied to enhance many swarm intelligence algorithms, such as evolutionary programming algorithm with Cauchy mutation [41], particle swarm optimization [42], the imperialist competitive algorithm with mutation operator [43] and so on. We adopt the inverse cumulative distribution function of Cauchy distribution, it is shown as Eq. (16).

$$F^{-1}(p; x_0, \gamma) = x_0 + \gamma \tan(\pi(p - \frac{1}{2})). \tag{16}$$

Finally, The Eq. (16) is adopted in GOA as Eq. (17).

$$X(t+1) = X(t) + \widehat{T}_d \tan(\pi(r - \frac{1}{2})). \tag{17}$$

where t is the current iteration; T_d has the same meaning as Eq. (2); r is a random number between 0 and 1. Eq. (17) disturbs the position of each grasshopper at each iteration.

3) OPERATION OF CC-GOA

The pseudocode of the CC-GOA algorithm is as follow:

Algorithm 1 Pseudocode of the CC-GOA Algorithm

1: Initialize the parameters of CC-GOA: population size (N), c_{max}, c_{min}, the current iteration t and maximum number of iteration t_{max}
2: A set of Logistic chaotic sequence is generated to initialize the swarm according to Eq. (14) and Eq. (15).
3: Set T as the best solution.
4: **while** $t < t_{max}$ **do**
5: Check the upper bound and lower bound of solutions.
6: Update c using Eq. (3).
7: The fitness value of individual is calculated according to the objective function.
8: **for** $i = 0 \rightarrow N$ **do**
9: Initialize the parameters of Cauchy mutation:
10: X_i^d is generated by Eq. (2)
11: The position of each individual is disturbed by Eq. (17).
12: **end for**
13: **end while**
14: Output the T

We can analyze the pseudocode of CC-GOA. In the preparation phase, the related parameters are defined and created; The CC-GOA runs and generates a set of the chaotic sequence using Eq. (14) and Eq. (15) by Logistic map. The search agents update their positions based on Eq. (2). In addition, CC-GOA disturbs the position of each individual according to Eq. (17) and the position of the best solution is updated in each iteration. The parameter c is generated by Eq. (3) and the fitness value is calculated by the objective function. Until the last iteration, The fitness value and position are outputted as the optimal solution. The GOA and CC-GOA are the two-layer loops, so the time complexity is $O(n^2)$. We can understand the general structure of the CC-GOA by the flow chart, it is listed as Fig. 5.

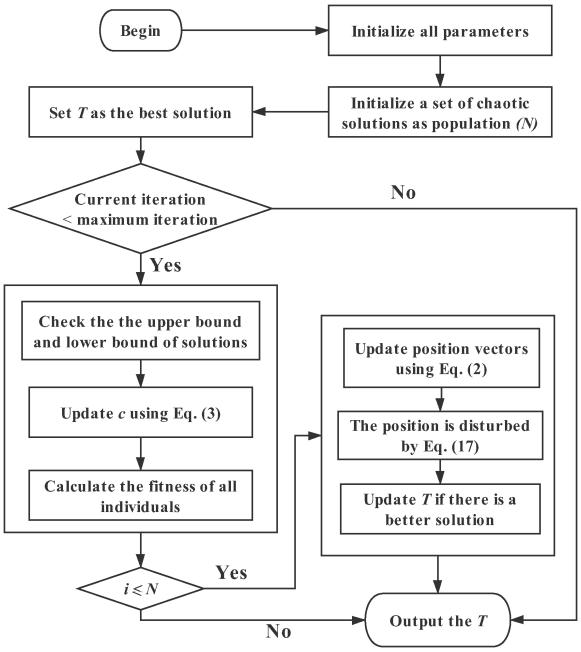

FIGURE 5. The flow chart of improved grasshopper optimization algorithm.

VI. EXPERIMENT: PERFORMANCE VERIFICATION OF ALGORITHM

The novel GOA algorithm discussed in the preceding sections is tested on sixteen benchmark functions in this section. The performance of this CC-GOA is evaluated in comparison with other six well-known algorithms. The experiments are performed on personal computer with Windows 10 Pro and 4G memory. The programs are written in MATLAB R2010a.

A. BENCHMARK FUNCTIONS

Eighteenth benchmark functions are used here for the numerical experiments. The benchmark functions are shown in Table 1. Type means the properties of functions, containing Unimodal or Multimodal; Dim is the dimension; f_{min} means the optimum value of functions.

B. COMPARISON WITH OTHER ALGORITHMS

In this subsection, best, mean and standard deviation values of objective function as three evaluation indexes are achieved by CC-GOA, OBLGOA [44], GOA [24] and Multi-Verse Optimizer (MVO) [45], Sine Cosine Algorithm (SCA) [46], Genetic Algorithm (GA), Differential Evolution (DE).

TABLE 1. Description of the benchmark optimization functions.

Test functions	Type	Search space	Dim	f_{min}
$f_1(x) = \sum_{i=1}^{D} x_i^2$	Unimodal	$[-100, 100]^D$	10	0
$f_2(x) = \sum_{i=1}^{D} \lvert x_i \rvert + \prod_{i=1}^{D} \lvert x_i \rvert$	Unimodal	$[-10, 10]^D$	10	0
$f_3(x) = \sum_{i=1}^{D} (\sum_{j=1}^{i} x_j)^2$	Unimodal	$[-100, 100]^D$	10	0
$f_4(x) = \max\{\lvert x_i \rvert, 1 \le i \le D\}$	Unimodal	$[-100, 100]^D$	10	0
$f_5(x) = \sum_{i=1}^{D-1} [100(x_i^2 - x_{i+1})^2 + (x_i - 1)^2]$	Unimodal	$[-30, 30]^D$	10	0
$f_6(x) = \sum_{i=1}^{n} i x_i^4 + random[0, 1]$	Unimodal	$[-1.28, 1.28]^D$	10	0
$f_7(x) = \sum_{i=1}^{n} ({x_i}^2 - 10\cos(2\pi x_i) + 10)$	Multimodal	$[-5.12, 5.12]^D$	10	0
$f_8(x) = -20\exp\left(-0.2\sqrt{\frac{1}{D}\sum_{i=1}^{D} x_i^2}\right)$ $-\exp\left(\frac{1}{D}\sum_{i=1}^{D}\cos(2\pi x_i)\right) + 20 + e$	Multimodal	$[-32, 32]^D$	10	0
$f_9(x) = \frac{1}{4000}\sum_{i=1}^{n} x_i^2 - \prod_{i=1}^{n}\cos\left(\frac{x_i}{\sqrt{i}}\right) + 1$	Multimodal	$[-600, 600]^D$	10	0
$f_{10}(x) = \frac{\pi}{D}\{10\sin^2(\pi y_1) + \sum_{i=1}^{D-1}(y_i - 1)^2[1 + 10\sin^2(\pi y_{i+1})]$ $+(y_n - 1)^2\} + \sum_{i=1}^{D} u(x_i, 10, 100, 4)$ $u(x_i, a, k, m) = \begin{cases} k(x_i - a)^m, & x_i > a \\ 0, & -a \le x_i \le a \\ k(-x_i - a)^m, & x < -a \end{cases}$	Multimodal	$[-50, 50]^D$	10	0
$f_{11}(x) = 0.1\{\sin^2(3\pi x_1) + \sum_{i=1}^{D}(x_i - 1)^2[1 + \sin^2(3\pi x_i + 1)]$ $+(x_n - 1)^2[1 + \sin^2(2\pi x_n)]\} + \sum_{i=1}^{D} u(x_i, 5, 100, 4)$	Multimodal	$[-50, 50]^D$	10	0
$f_{12}(x) = \left(\frac{1}{500} + \sum_{j=1}^{25}\frac{1}{j + \sum_{i=1}^{2}(x_i - a_{ij})^6}\right)^{-1}$	Multimodal	$[-65.536, 65.536]^D$	2	1
$f_{13}(x) = \sum_{i=1}^{11}\left[a_i - \frac{x_1(b_i^2 + b_i x_2)}{b_i^2 + b_i x_3 + x_4}\right]^2$	Multimodal	$[-5, 5]^D$	4	0.00030
$f_{14}(x) = -\sum_{i=1}^{4} c_i \exp(-\sum_{j=1}^{6} a_{ij}(x_j - p_{ij})^2)$	Multimodal	$[0, 1]^D$	6	-3.32
$f_{15}(x) = -\sum_{i=1}^{7}[(x - a_i)(x - a_i)^T + c_i]^{-1}$	Multimodal	$[0, 10]^D$	4	-10.4028
$f_{16}(x) = \sum_{i=1}^{n} -x_i \sin(\sqrt{\lvert x_i \rvert})$	Multimodal	$[-500, 500]^D$	10	-418.98*10

The experimental settings are as follows: the number of the swarm size is taken as 50, the maximum number of iteration is set as 100, the dimension size is similar to the Dim of Table 1, each experiment is conducted for 30 times independently.

As revealed in Table 2, the bold fonts are the optimal performance of several algorithms. In the comparison between the three GOA algorithms, CC-GOA performs better than GOA and OBL-GOA on the nine functions ($f_1, f_2, f_3, f_4, f_7, f_8, f_9, f_{10}, f_{11}$), followed by OBL-GOA and GOA. CC-GOA and OBL-GOA algorithms have similar performance on five functions($f_5, f_6, f_{12}, f_{13}, f_{16}$) and OBL-GOA obtains better standard deviation value on f_{14} and f_{15}. It can be known that CC-GOA have good search accuracy between the three GOA algorithms.

In terms of best function values, GA does well on the function f_{10} and CC-GOA obtains the optimal solution on the rest fifteen functions; from best and mean values we know, seven algorithms perform similarly on the functions (f_{13} and f_{14}), SCA, GA and OBL-GOA get respectively the smaller standard deviation value on f_{13}, f_{14} and f_{15}, but the solution obtained by CC-GOA is more stable than other six algorithms on the rest thirteen functions; take into three evaluation indexes consideration, the CC-GOA has a significant optimization on seven functions ($f_1, f_2, f_3, f_4, f_7, f_8, f_9$) and

TABLE 2. Comparison of CC-GOA OBL-GOA GOA MVO SCA GA DE.

Fuction	Index	CC-GOA	OBL-GOA [44]	GOA [24]	MVO [45]	SCA [46]	GA	DE
f_1	Best	$\mathbf{1.77E-17}$	$1.31E-08$	$2.68E-02$	$1.54E-01$	$4.02E-02$	$9.12E-03$	$9.91E-02$
	Mean	$\mathbf{9.38E-13}$	$3.00E-06$	$1.28E-01$	$3.95E-01$	$7.16E+00$	$1.90E-01$	$4.00E-01$
	Std	$\mathbf{1.78E-12}$	$9.84E-06$	$6.79E-02$	$1.68E-01$	$1.23E+01$	$2.17E-01$	$2.15E-01$
f_2	Best	$\mathbf{6.97E-09}$	$2.45E-05$	$8.75E-03$	$7.77E-02$	$1.35E-03$	$3.31E-04$	$5.07E-02$
	Mean	$\mathbf{2.38E-07}$	$9.38E-05$	$2.32E-01$	$1.99E-01$	$1.03E-01$	$1.15E-02$	$8.42E-02$
	Std	$\mathbf{3.04E-07}$	$6.43E-05$	$2.04E-01$	$8.79E-02$	$8.06E-02$	$1.26E-02$	$2.27E-02$
f_3	Best	$\mathbf{1.84E-19}$	$3.10E-07$	$4.37E-01$	$5.55E-01$	$5.60E+00$	$8.33E+01$	$9.14E+02$
	Mean	$\mathbf{6.97E-12}$	$2.97E-04$	$5.87E+00$	$2.86E+00$	$2.46E+02$	$5.57E+02$	$2.08E+03$
	Std	$\mathbf{2.33E-11}$	$4.03E-04$	$5.09E+00$	$2.84E+00$	$5.42E+02$	$4.58E+02$	$6.10E+02$
f_4	Best	$\mathbf{1.08E-09}$	$4.30E-05$	$7.89E-02$	$2.40E-01$	$3.56E-01$	$1.13E+00$	$5.09E+00$
	Mean	$\mathbf{5.33E-07}$	$3.36E-04$	$3.12E-01$	$5.08E-01$	$4.34E+00$	$4.95E+00$	$8.39E+00$
	Std	$\mathbf{8.32E-07}$	$1.74E-04$	$2.01E-01$	$2.28E-01$	$3.73E+00$	$3.78E+00$	$2.05E+00$
f_5	Best	$\mathbf{8.34E+00}$	$\mathbf{8.47E+00}$	$\mathbf{8.26E+00}$	$\mathbf{8.82E+00}$	$1.42E+01$	$\mathbf{8.49E+00}$	$5.74E+01$
	Mean	$\mathbf{8.84E+00}$	$\mathbf{8.80E+00}$	$1.57E+02$	$3.40E+02$	$4.01E+02$	$1.22E+02$	$1.65E+02$
	Std	$\mathbf{1.52E-01}$	$\mathbf{1.47E-01}$	$3.48E+02$	$7.89E+02$	$7.68E+02$	$2.37E+02$	$6.19E+01$
f_6	Best	$\mathbf{7.39E-05}$	$\mathbf{5.35E-05}$	$5.66E-03$	$2.82E-03$	$1.93E-03$	$3.41E-03$	$9.66E-03$
	Mean	$\mathbf{5.27E-04}$	$\mathbf{2.15E-04}$	$2.38E-02$	$1.25E-02$	$2.30E-02$	$2.15E-02$	$3.33E-02$
	Std	$\mathbf{3.90E-04}$	$\mathbf{1.18E-04}$	$2.20E-02$	$6.32E-03$	$1.77E-02$	$1.29E-02$	$1.13E-02$
f_7	Best	$\mathbf{4.26E-14}$	$5.74E-09$	$3.98E+00$	$6.13E+00$	$1.24E+00$	$2.51E+00$	$9.70E+00$
	Mean	$\mathbf{2.09E-12}$	$2.59E-08$	$2.24E+01$	$2.70E+01$	$1.81E+01$	$6.26E+00$	$1.60E+01$
	Std	$\mathbf{6.28E-12}$	$2.40E-08$	$1.27E+01$	$1.43E+01$	$1.46E+01$	$2.46E+00$	$3.29E+00$
f_8	Best	$\mathbf{1.93E-09}$	$4.45E-05$	$1.44E-01$	$2.29E-01$	$1.55E-01$	$1.03E-02$	$2.82E-01$
	Mean	$\mathbf{4.56E-07}$	$2.02E-04$	$1.41E+00$	$1.01E+00$	$3.86E+00$	$2.59E-01$	$6.93E-01$
	Std	$\mathbf{9.91E-07}$	$1.38E-04$	$8.87E-01$	$6.44E-01$	$6.08E+00$	$3.95E-01$	$3.66E-01$
f_9	Best	$\mathbf{7.77E-16}$	$9.05E-06$	$1.45E-01$	$4.05E-01$	$1.94E-02$	$5.45E-02$	$3.80E-01$
	Mean	$\mathbf{1.77E-11}$	$9.25E-05$	$3.17E-01$	$6.86E-01$	$7.33E-01$	$2.61E-01$	$6.66E-01$
	Std	$\mathbf{3.19E-11}$	$8.99E-05$	$1.44E-01$	$1.65E-01$	$2.49E-01$	$9.68E-01$	$1.23E-01$
f_{10}	Best	$8.60E-04$	$1.82E-03$	$1.38E-02$	$8.87E-03$	$1.56E-01$	$\mathbf{1.89E-06}$	$2.16E-02$
	Mean	$\mathbf{3.57E-02}$	$\mathbf{2.11E-02}$	$1.27E+00$	$4.95E-01$	$1.50E+00$	$\mathbf{3.28E-02}$	$\mathbf{3.63E-02}$
	Std	$\mathbf{3.04E-02}$	$\mathbf{1.31E-02}$	$1.32E+00$	$6.10E-01$	$1.28E+00$	$\mathbf{9.11E-02}$	$\mathbf{2.31E-02}$
f_{11}	Best	$\mathbf{5.64E-04}$	$1.60E-02$	$4.17E-03$	$1.14E-02$	$4.46E-01$	$\mathbf{7.72E-04}$	$2.20E-02$
	Mean	$\mathbf{4.93E-02}$	$\mathbf{6.93E-02}$	$\mathbf{3.54E-02}$	$\mathbf{4.34E-02}$	$1.58E+00$	$\mathbf{2.63E-02}$	$\mathbf{7.85E-02}$
	Std	$\mathbf{4.79E-02}$	$\mathbf{3.97E-02}$	$\mathbf{2.28E-02}$	$\mathbf{2.45E-02}$	$2.24E+00$	$\mathbf{2.60E-02}$	$\mathbf{2.76E-02}$
f_{12}	Best	$\mathbf{9.98E-01}$	$\mathbf{9.98E-01}$	$\mathbf{9.98E-01}$	$\mathbf{9.98E-01}$	$\mathbf{9.98E-01}$	$\mathbf{9.98E-01}$	$\mathbf{9.98E-01}$
	Mean	$\mathbf{3.27E+00}$	$\mathbf{1.26E+00}$	$\mathbf{1.36E+00}$	$\mathbf{2.62E+00}$	$\mathbf{2.41E+00}$	$\mathbf{1.08E+00}$	$\mathbf{1.03E+00}$
	Std	$\mathbf{2.25E-01}$	$\mathbf{4.40E-01}$	$\mathbf{6.53E-01}$	$3.58E+00$	$1.09E+00$	$\mathbf{2.43E-01}$	$\mathbf{1.66E-01}$
f_{13}	Best	$\mathbf{3.15E-04}$	$\mathbf{3.74E-04}$	$\mathbf{7.40E-04}$	$\mathbf{5.11E-04}$	$\mathbf{4.04E-04}$	$\mathbf{7.14E-04}$	$\mathbf{7.09E-04}$
	Mean	$\mathbf{1.26E-03}$	$\mathbf{1.85E-03}$	$\mathbf{3.71E-03}$	$\mathbf{4.35E-03}$	$\mathbf{1.25E-03}$	$\mathbf{3.03E-03}$	$\mathbf{1.25E-03}$
	Std	$3.72E-03$	$2.73E-03$	$6.18E-03$	$6.99E-03$	$\mathbf{5.10E-04}$	$4.44E-03$	$\mathbf{4.44E-04}$
f_{14}	Best	$\mathbf{-3.86E+00}$	$\mathbf{-3.86E+00}$	$\mathbf{-3.86E+00}$	$\mathbf{-3.86E+00}$	$\mathbf{-3.86E+00}$	$\mathbf{-3.86E+00}$	$\mathbf{-3.86E+00}$
	Mean	$\mathbf{-3.62E+00}$	$\mathbf{-3.86E+00}$	$\mathbf{-3.86E+00}$	$\mathbf{-3.86E+00}$	$\mathbf{-3.85E+00}$	$\mathbf{-3.86E+00}$	$\mathbf{-3.86E+00}$
	Std	$2.69E-01$	$7.50E-04$	$3.20E-02$	$7.52E-05$	$6.98E-03$	$\mathbf{2.28E-08}$	$1.45E-04$
f_{15}	Best	$\mathbf{-10.32E+00}$	$\mathbf{-5.13E+00}$	$\mathbf{-2.75E+00}$	$-1.04E+01$	$\mathbf{-4.95E+00}$	$\mathbf{-9.23E+00}$	$-1.04E+01$
	Mean	$\mathbf{-7.35E+00}$	$-1.03E+01$	$\mathbf{-8.15E+00}$	$\mathbf{-6.62E+00}$	$\mathbf{-2.84E+00}$	$\mathbf{-4.36E+00}$	$\mathbf{-8.61E+00}$
	Std	$1.83E+00$	$\mathbf{8.67E-01}$	$3.26E+00$	$3.73E+00$	$1.30E+00$	$1.93E+00$	$2.03E+00$
f_{16}	Best	$\mathbf{-4.17E+03}$	$\mathbf{-3.64E+03}$	$\mathbf{-3.52E+03}$	$\mathbf{-3.72E+03}$	$\mathbf{-2.47E+03}$	$\mathbf{-4.07E+03}$	$\mathbf{-3.92E+03}$
	Mean	$\mathbf{-3.65E+03}$	$\mathbf{-3.02E+03}$	$\mathbf{-2.83E+03}$	$\mathbf{-2.82E+03}$	$\mathbf{-1.96E+03}$	$\mathbf{-3.63E+03}$	$\mathbf{-3.55E+03}$
	Std	$\mathbf{7.90E+02}$	$\mathbf{3.46E+02}$	$\mathbf{3.22E+02}$	$\mathbf{3.52E+02}$	$\mathbf{1.94E+02}$	$\mathbf{2.01E+02}$	$\mathbf{1.88E+02}$

CC-GOA even optimizes 10^{12} on the function f_3 than the rest algorithms. In summary, CC-GOA obtains better quality solution than other six algorithms. It means that CC-GOA has fine convergence and search accuracy.

As illustrated in Fig. 6, the convergence curves of two unimodal functions and two multimodal functions are selected as representative from sixteen benchmark functions. Comparison of the performance of seven algorithms between unimodal functions and multimodal functions. Fig. 6-a and Fig. 6-b are the unimodal functions with only a local optimum (peak) in the interval. Fig. 6-a shows that the convergence rate of CC-GOA is much faster than the other six algorithms, followed by OBL-GOA, the slowest is SCA. MVO get the low accuracy solution and CC-GOA can find the more accuracy value; Fig. 6-b reveals that the search accuracy of OBL-GOA appears to decline, but CC-GOA still has good convergence rate and accuracy; Fig. 6-c and Fig. 6-d are the multimodal functions, which surround the global optimum with a large number of local optimal points in the interval.

As the complexity of the objective function increases, the search ability of all algorithms degrades. Fig. 6-c indicates that DE, SCA and GOA, MVO have similar search accuracy, CC-GOA performs well; Fig. 6-d exposes that GA has fine convergence speed, while CC-GOA can obtain the relatively precision solution. In conclusion, CC-GOA has fast convergence rate and high accuracy.

VII. APPLICATION: OPTIMIZATION OF PIEZORESISTIVE ACCELERATION SENSOR

The CC-GOA algorithm with 50 search agents and a maximum of 200 iterations is employed to optimize this problem, each experiment is repeated 20 times independently on

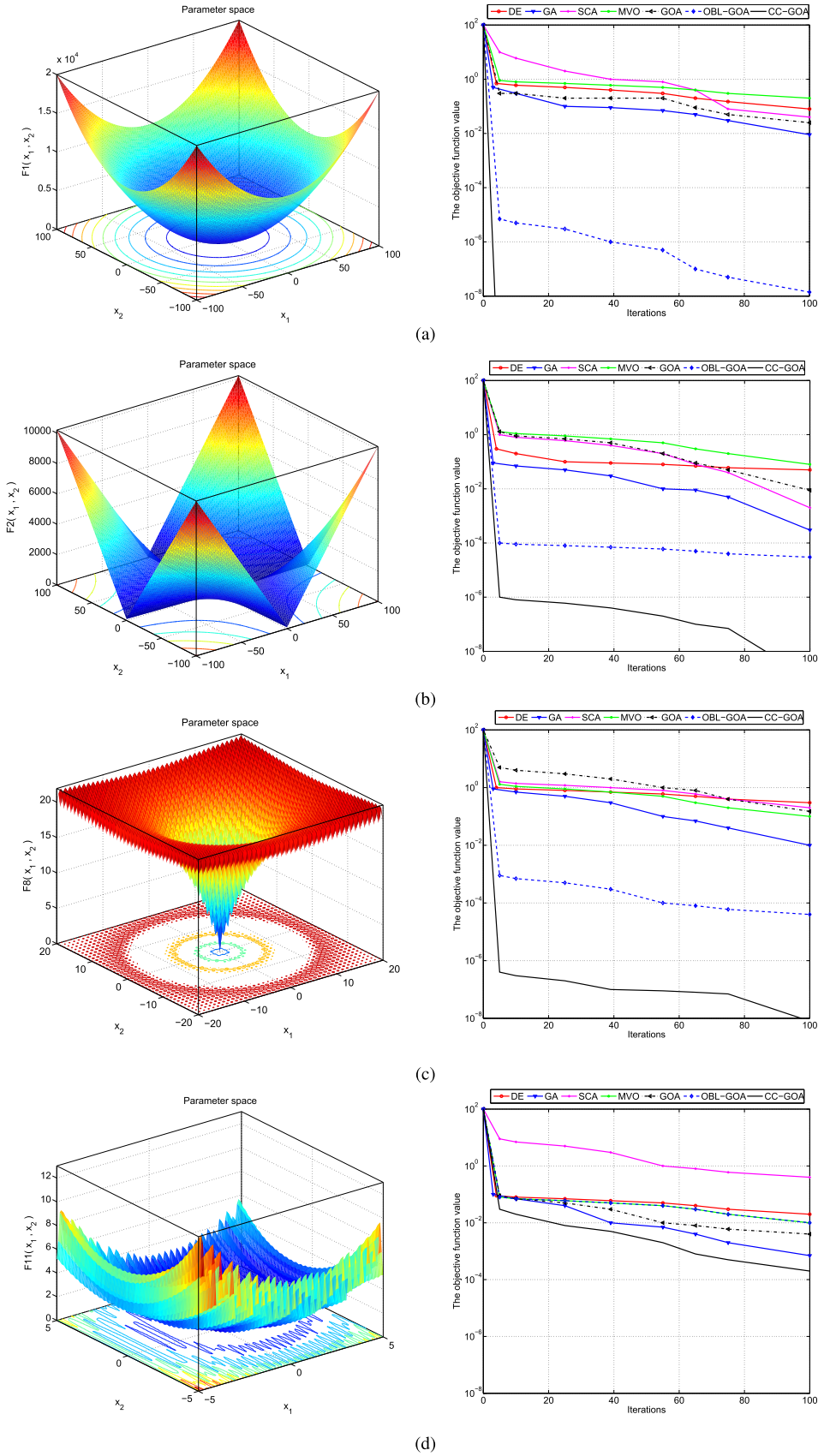

FIGURE 6. Convergence curves of seven algorithms on the benchmark functions. (a) Results of unimodal function f_1. (b) Results of munimodal function f_2. (c) Results of munimodal function f_8. (d) (d) Results of munimodal function f_{11}.

TABLE 3. Results of two methods on *Si*.

$Si \quad E_1 = 119.5GPa$								
	CC-GOA				GOA			
$m(g)$	$b(\mu m)$	$l(\mu m)$	$h(\mu m)$	$\eta(\mu m/g)$	$b(\mu m)$	$l(\mu m)$	$h(\mu m)$	$\eta(\mu m/g)$
$0 \sim 100$	80	354	30	8.23E-04	231	693	126	1.05E-04
$100 \sim 200$	80	148	52	2.93E-04	389	181	56	2.64E-05
$200 \sim 300$	160	715	63	9.14E-04	228	304	30	7.87E-04
$300 \sim 400$	87	354	34	9.62E-04	525	447	94	1.52E-04
$400 \sim 500$	146	322	30	9.24E-04	80	148	30	6.67E-04
$500 \sim 600$	80	150	30	7.18E-04	223	264	71	2.14E-04

TABLE 4. Results of two methods on *Al*.

$Al \quad E_2 = 70GPa$								
	CC-GOA				GOA			
$m(g)$	$b(\mu m)$	$l(\mu m)$	$h(\mu m)$	$\eta(\mu m/g)$	$b(\mu m)$	$l(\mu m)$	$h(\mu m)$	$\eta(\mu m/g)$
$0 \sim 100$	80	354	30	9.01E-04	326	203	30	1.42E-04
$100 \sim 200$	80	148	30	4.22E-04	223	264	71	9.40E-05
$200 \sim 300$	91	201	30	7.59E-04	129	408	100	3.52E-04
$300 \sim 400$	160	715	64	9.67E-04	492	752	76	7.75E-04
$400 \sim 500$	952	674	90	4.43E-04	280	378	123	1.39E-04
$500 \sim 600$	80	403	30	1.00E-03	325	534	31	9.95E-04

TABLE 5. Results of CC-GOA on fixed mass.

CC-GOA								
	$Si \quad E_1 = 119.5GPa$				$Al \quad E_2 = 70GPa$			
$m(g)$	$b(\mu m)$	$l(\mu m)$	$h(\mu m)$	$\eta(\mu m/g)$	$b(\mu m)$	$l(\mu m)$	$h(\mu m)$	$\eta(\mu m/g)$
100	225	438	30	2.88E-04	80	170	30	4.70E-04
200	80	405	30	1.21E-04	80	102	38	2.85E-04
300	182	154	30	4.71E-05	325	506	118	2.17E-04
400	352	373	68	9.67E-05	80	920	32	3.71E-04
500	130	414	47	5.31E-04	80	314	35	9.83E-04
600	102	575	82	4.21E-04	522	800	30	9.95E-03

two different materials of the mass block, which are respectively *Si* ($E_1 = 119.5GPa$), *Al* ($E_2 = 70GPa$).

A. DESIGN ON DIVERSE MASS

The mass of the mass block is set in 0∼100g, 100∼200g, 200∼300g and 300∼400g, 400∼500g, 500∼600g on two different materials that large difference in elastic modulus. The results is shown in Table 3 and Table 4.

Three structural parameters are optimized and the structural sensitivity of the piezoresistive acceleration sensor is relatively optimal in CC-GOA than GOA. As the mass of the *Si* increases, the structural sensitivity that CC-GOA designs has a little change on 200∼500g and changes a lot on 0∼300g, 400∼600g; the value of the structural sensitivity calculated by GOA exists large fluctuation at all stages; As revealed in Table 4, the results are designed by CC-GOA and GOA based on the material of *Al*. The elastic modulus of *Si* is higher than *Al*, the change affects the structural sensitivity. The GOA design better on *Al* than *Si*, Whereas, the CC-GOA optimize the structural sensitivity better than GOA. Comparison with *Si*, the optimization results of CC-GOA declines on 200∼300g, 400∼500g, but increases on the other four scopes.

B. DESIGN ON FIXED MASS

CC-GOA runs on the mass block that is defined in 100g, 200g, 300g and 400g, 500g, 600g. As indicated in Table 5, when the mass is fixed, the sensitivity is designed better on *Al* than *Si*. With the mass increases at a step size of 100g, the sensitivity of *Si* goes down and then it goes up, the sensitivity of *Al* is relatively stable. In *Si*, the CC-GOA obtains the optimal value on 500g and the worst value on 300g. As for *Al*, the CC-GOA even obtain 10^{-3} and optimize 10^{1} than *Si* on 600g. Three structural parameters are designed, *b* and *h* are relatively small, *l* is relatively large. Compared to Table 3 and Table 4, the sensitivity of *Si* declines a little, the sensitivity of *Al* droops on 0∼400g and ascends on 400∼600g, but the CC-GOA can find the optimal solution on 600g. In summary, CC-GOA optimizes the three structural parameters and obtains the relatively optimal structural sensitivity of piezoresistive acceleration sensor on two different materials.

VIII. CONCLUSION

At present, the Internet of things is constantly evolving, sensors are also constantly upgrading as the basic components. In this article, the piezoresistive acceleration sensor of the cantilever beam is considered as the research object, the structure of piezoresistive acceleration sensor contains four beams and mass block. The structural sensitivity is the key index to evaluate the design of the piezoresistive acceleration sensor. The mathematical design model for the structural sensitivity of piezoresistive acceleration sensor is proposed and a novel method that combines chaos strategy and Cauchy mutation on grasshopper optimization algorithm is introduced to optimize the design of the sensor. First of all, the method (CC-GOA) is compared with six well-

known algorithms to verify the search ability of CC-GOA on sixteen benchmark functions, the experimental results show CC-GOA has fast convergence rate and finds the solution with high precision. Then CC-GOA is employed to optimize the structural sensitivity of piezoresistive acceleration sensor on two different materials. With the increase of the mass, CC-GOA still obtains the relatively optimal structural sensitivity. It means that the novel method based on improved grasshopper optimization algorithm for the optimization of the piezoresistive acceleration sensor is effective and desirable.

In future work, the research of piezoresistive acceleration sensor will be further extended to enhance the sensitivity. Furthermore, swarm intelligent algorithm is applied in other optimization problems of the industrial Internet of Thing, such as layout of weigh-in-motion sensor, wireless sensor networks localization, etc.

REFERENCES

[1] K. Ding and P. Jiang, "RFID-based production data analysis in an IoT-enabled smart job-shop," *IEEE/CAA J. Automatica Sinica*, vol. 5, no. 1, pp. 128–138, Jan. 2018.

[2] M. T. Arafin, D. Anand, and G. Qu, "A low-cost GPS spoofing detector design for Internet of Things (IoT) applications," in *Proc. ACM Great Lakes Symp.*, May 2017, pp. 161–166.

[3] L. Biqing, Z. Shiyong, and Q. Ming, "Research on picking identification and positioning system based on IOT," *Int. J. Online Eng.*, vol. 14, no. 7, pp. 149–160, 2018.

[4] D. C. Yacchirema, D. Sarabia-Jácome, C. E. Palau, and M. Esteve, "A smart system for sleep monitoring by integrating IoT with big data analytics," *IEEE Access*, vol. 6, pp. 35988–36001, 2018.

[5] F. Tao, Y. Zuo, L. Da Xu, and L. Zhang, "IoT-based intelligent perception and access of manufacturing resource toward cloud manufacturing," *IEEE Trans. Ind. Informat.*, vol. 10, no. 2, pp. 1547–1557, May 2014.

[6] H. C. Hwang, J. S. Park, and J. G. Shon, "Design and implementation of a reliable message transmission system based on MQTT protocol in IoT," *Wireless Pers. Commun.*, vol. 91, no. 4, pp. 1765–1777, 2016.

[7] G. M. Milis, C. G. Panayiotou, and M. M. Polycarpou, "SEMIoTICS: Semantically-enhanced IoT-enabled intelligent control systems," *IEEE Internet Things J.*, to be published. [Online]. Available: http://ieeexplore.ieee.org/stamp/stamp.jsp?tp=&arnumber=8106780&isnumber=6702522, doi: 10.1109/JIOT.2017.2773200.

[8] S. Rodríguez-Valenzuela, J. A. Holgado-Terriza, J. M. Gutiérrez-Guerrero, and J. L. Muros-Cobos, "Distributed service-based approach for sensor data fusion in IoT environments," *Sensors*, vol. 14, no. 10, pp. 19200–19228, 2014.

[9] T. Qu, S. P. Lei, Z. Z. Wang, D. X. Nie, X. Chen, and G. Q. Huang, "IoT-based real-time production logistics synchronization system under smart cloud manufacturing," *Int. J. Adv. Manuf. Technol.*, vol. 84, nos. 1–4, pp. 147–164, 2016.

[10] A. Al-Dweik, R. Muresan, M. Mayhew, and M. Lieberman, "IoT-based multifunctional scalable real-time enhanced road side unit for intelligent transportation systems," in *Proc. IEEE 30th Can. Conf. Elect. Comput. Eng. (CCECE)*, May 2017, pp. 1–6.

[11] D. Minoli, K. Sohraby, and B. Occhiogrosso, "IoT considerations, requirements, and architectures for smart buildings—Energy optimization and next-generation building management systems," *IEEE Internet Things J.*, vol. 4, no. 1, pp. 269–283, Feb. 2017.

[12] M. R. Palattella, N. Accettura, L. A. Grieco, G. Boggia, M. Dohler, and T. Engel, "On optimal scheduling in duty-cycled industrial IoT applications using IEEE802.15.4e TSCH," *IEEE Sensors J.*, vol. 13, no. 10, pp. 3655–3666, Oct. 2013.

[13] S. Vetrivel, R. Mathew, and A. R. Sankar, "Design and optimization of a doubly clamped piezoresistive acceleration sensor with an integrated silicon nanowire piezoresistor," *Microsyst. Technol.*, vol. 23, no. 8, pp. 3525–3536, 2016.

[14] M. Messina, J. Njuguna, and C. Palas, "Mechanical structural design of a MEMS-based piezoresistive accelerometer for head injuries monitoring: A computational analysis by increments of the sensor mass moment of inertia," *Sensors*, vol. 18, no. 1, p. 289, 2018.

[15] F. Liu *et al.*, "Optimal design of high-g MEMS piezoresistive accelerometer based on Timoshenko beam theory," *Microsyst. Technol.*, vol. 24, no. 2, pp. 855–867, 2018.

[16] A. Kazama, T. Aono, and R. Okada, "High shock-resistant design for wafer-level-packaged three-axis accelerometer with ring-shaped beam," *J. Microelectromech. Syst.*, vol. 27, no. 2, pp. 355–364, Apr. 2018.

[17] Z. Ghemari, "Study and analysis of the piezoresistive accelerometer stability and improvement of their performances," *Int. J. Syst. Assurance Eng. Manage.*, vol. 8, pp. 1520–1526, Nov. 2017.

[18] R. S. Jakati, K. B. Balavalad, and B. G. Sheeparamatti, "Sensitivity enhancement in piezoresistive micro-pressure sensor using perforated diaphragm," in *Proc. IEEE 2nd Int. Conf. Recent Trends Electron., Inf. Commun. Technol. (RTEICT)*, May 2017, pp. 396–399.

[19] K. Hari, S. K. Verma, I. R. P. Krishna, and V. Seena, "Out-of-plane dual flexure MEMS piezoresistive accelerometer with low cross axis sensitivity," *Microsyst. Technol.*, vol. 24, no. 5, pp. 2437–2444, 2017.

[20] M. Defdaf, Z. Ghemari, A. E. Hadjaj, and S. Saad, "Improvement of method queues by progress of the piezoresistive accelerometer parameters," *J. Adv. Manuf. Syst.*, vol. 16, no. 3, pp. 227–235, 2017.

[21] Z. Ghemari and S. Saad, "Simulation and experimental validation of new model for the piezoresistive accelerometer displacement," *Sensor Lett.*, vol. 15, no. 2, pp. 132–135, 2017.

[22] P. Wang *et al.*, "A piezoresistive micro-accelerometer with high frequency response and low transverse effect," *Meas. Sci. Technol.*, vol. 28, no. 1, p. 015103, 2017.

[23] Y. Xu, L. Zhao, Z. Jiang, J. Ding, N. Peng, and Y. Zhao, "A novel piezoresistive accelerometer with SPBs to improve the tradeoff between the sensitivity and the resonant frequency," *Sensors*, vol. 16, no. 2, p. 210, 2016.

[24] S. Saremi, S. Mirjalili, and A. Lewis, "Grasshopper optimisation algorithm: Theory and application," *Adv. Eng. Softw.*, vol. 105, pp. 30–47, Mar. 2017.

[25] A. A. Heidari. H. Faris, I. Aljarah, and S. Mirjalili, "An efficient hybrid multilayer perceptron neural network with grasshopper optimization," in *Soft Computing*. Springer, 2018, pp. 1–18, doi: 10.1007/s00500-018-3424-2.

[26] N. Rajput, V. Chaudhary, H. M. Dubey, and M. Pandit, "Optimal generation scheduling of thermal system using biologically inspired grasshopper algorithm," in *Proc. 2nd Int. Conf. Telecommun. Netw.*, Aug. 2017, pp. 1–6.

[27] X. Zhang, Q. Miao, H. Zhang, and L. Wang, "A parameter-adaptive VMD method based on grasshopper optimization algorithm to analyze vibration signals from rotating machiner," *Mech. Syst. Signal Process.*, vol. 108, pp. 58–72, Aug. 2018.

[28] A. Hamad, E. H. Houssein, A. E. Hassanien, and A. A. Fahmy, "Hybrid grasshopper optimization algorithm and support vector machines for automatic seizure detection in EEG signals," in *Proc. Int. Conf. Adv. Mach. Learn. Technol. Appl.*, Jan. 2018, pp. 82–91.

[29] A. A. Amaireh, A. Alzoubi, and N. I. Dib, "Design of linear antenna arrays using antlion and grasshopper optimization algorithms," in *Proc. IEEE Jordan Conf. Appl. Electr. Eng. Comput. Technol.*, Oct. 2017, pp. 1–6.

[30] S. Z. Mirjalili, S. Mirjalili, S. Saremi, H. Faris, and I. Aljarah, "Grasshopper optimization algorithm for multi-objective optimization problems," *Appl. Intell.*, vol. 48, no. 4, pp. 805–820, 2018.

[31] M. Mafarja *et al.*, "Evolutionary population dynamics and grasshopper optimization approaches for feature selection problems," *Knowl.-Based Syst.*, no. 145, pp. 25–45, Apr. 2017.

[32] S. Arora and P. Anand, "Chaotic grasshopper optimization algorithm for global optimization," in *Neural Computing and Applications*, no. 6. Springer, 2018, pp. 1–21, doi: 10.1007/s00521-018-3343-2.

[33] D. Potnuru and A. S. L. V. Tummala, "Implementation of grasshopper optimization algorithm for controlling a BLDC motor drive," in *Soft Computing in Data Analytics*. Springer, 2018, pp. 369–376, doi: 10.1007/978-981-13-0514-6_37.

[34] M. Mafarja, I. Aljarah, A. A. Heidari, A. I. Hammouri, H. Faris, and A. Al-Zoubi, "Chronological grasshopper optimization algorithm-based gene selection and cancer classification," *J. Adv. Res. Dyn. Control Syst.*, vol. 10, no. 3, pp. 80–94, 2018.

[35] C. Wagner, J. Schuster, and T. Gessner, "DFT investigations of the piezoresistive effect of carbon nanotubes for sensor application," *Phys. Status Solidi*, vol. 249, no. 12, pp. 2450–2453, 2012.
[36] T. Miao, D. Xiao, Q. Li, Z. Hou, and X. Wu, "A 4 mm^2 double differential torsional MEMS accelerometer based on a double-beam configuration," *Sensors*, vol. 17, no. 10, p. 2264, 2017.
[37] K. Chen, F. Zhou, and A. Liu, "Chaotic dynamic weight particle swarm optimization for numerical function optimization," *Knowl.-Based Syst.*, vol. 139, pp. 23–40, Jan. 2018.
[38] M. Moradi, S. Nejatian, H. Parvin, and V. Rezaie, "CMCABC: Clustering and memory-based chaotic artificial bee colony dynamic optimization algorithm," *Int. J. Inf. Technol. Decis. Making*, vol. 17, no. 4, pp. 1007–1046, 2018.
[39] G. Kaur and S. Arora, "Chaotic whale optimization algorithm," *J. Comput. Des. Eng.*, vol. 5, no. 3, pp. 275–284, 2018.
[40] D. Navarro-Urrios *et al.*, "Nonlinear dynamics and chaos in an optomechanical beam," *Nature Commun.*, vol. 8, Apr. 2017, Art. no. 14965.
[41] M. Hajebi, A. Tavakoli, and A. Hoorfar, "Frequency domain inverse profiling of buried dielectric elliptical-cylindrical objects using evolutionary programming," *IEEE Geosci. Remote Sens. Lett.*, vol. 15, no. 4, pp. 503–507, Apr. 2018.
[42] Y. Zou, P. X. Liu, C. Yang, C. Li, and Q. Cheng, "Collision detection for virtual environment using particle swarm optimization with adaptive cauchy mutation," *Cluster Comput.*, vol. 20, no. 2, pp. 1765–1774, 2017.
[43] S. Xu, Y. Wang, and P. Lu, "Improved imperialist competitive algorithm with mutation operator for continuous optimization problems," *Neural Comput. Appl.*, vol. 28, no. 7, pp. 1667–1682, 2017.
[44] A. A. Ewees, M. A. Elaziz, and E. H. Houssein, "Improved grasshopper optimization algorithm using opposition-based learning," *Expert Syst. Appl.*, vol. 1112, pp. 156–172, Dec. 2018.
[45] S. Mirjalili, S. M. Mirjalili, and A. Hatamlou, "Multi-verse optimizer: A nature-inspired algorithm for global optimization," *Neural Comput. Appl.*, vol. 27, no. 2, pp. 495–513, 2016.
[46] S. Mirjalili, "SCA: A sine cosine algorithm for solving optimization problems," *Knowl.-Based Syst.*, vol. 96, pp. 120–133, Mar. 2016.

CHEN DONG received the B.S. and M.S. degrees from the College of Mathematics and Computer Science, Fuzhou University, China, in 2002 and 2005, respectively, and the Ph.D. degree in computer science from the Computer School, Wuhan University, China, in 2011. She was a Visiting Researcher with the University of California at Los Angeles, Los Angeles, from 2015 to 2016. She is currently an Assistant Professor with the College of Mathematics and Computer Science, Fuzhou University. Her research interests include artificial intelligence, hardware security, intelligent computing, and integrated circuit physical design.

YIN YE received the B.S. degree in civil engineering from the Jiangxi University of Science and Technology, China, in 2017. He is currently pursuing the master's degree with the Fujian Provincial Key Laboratory of Information Security of Network Systems, College of Mathematics and Computer Science, Fuzhou University. His research interests include intelligent computing and engineering application.

XIMENG LIU received the B.Sc. degree in electronic engineering and the Ph.D. degree in cryptography from Xidian University, Xi'an, China, in 2010 and 2015, respectively. He is currently a Full Professor with the College of Mathematics and Computer Science, Fuzhou University. He is also a Research Fellow with the School of Information System, Singapore Management University, Singapore. He has published more than 100 papers in the topics of cloud security and big data security, including papers in the IEEE TRANSACTIONS ON COMPUTERS, the IEEE TRANSACTIONS ON INDUSTRIAL INFORMATICS, the IEEE TRANSACTIONS ON DEPENDABLE AND SECURE COMPUTING, the IEEE TRANSACTIONS ON SERVICE COMPUTING, and the IEEE INTERNET OF THINGS JOURNAL. He served as a Program Committee for several conferences, such as the 17th IEEE International Conference on Trust, Security and Privacy in Computing and Communications, the 2017 IEEE Global Communications Conference, and the 2016 IEEE Global Communications Conference. His research interests include cloud security, applied cryptography, and big data security. He is a member of the IEEE, ACM, and CCF. His awards include "Minjiang Scholars" Distinguished Professor, "Qishan Scholars" in Fuzhou University, and the ACM SIGSAC China Rising Star Award in 2018. He served as a Lead Guest Editor for *Wireless Communications and Mobile Computing*.

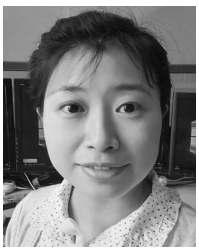

YANG YANG received the B.Sc. and Ph.D. degrees from Xidian University, Xi'an, China, in 2006 and 2011, respectively. She has been a Research Fellow (Postdoctor) under the supervision of R. H. Deng in Singapore Management University. She is currently an Associate Professor with the College of Mathematics and Computer Science, Fuzhou University. She has published more than 60 papers in the IEEE TIFS, the IEEE TDSC, the IEEE TSC, the IEEE TCC, and the IEEE TII. Her research interests include information security and privacy protection.

WENZHONG GUO received the B.S. and M.S degrees in computer science and the Ph.D. degree in communication and information system from Fuzhou University, Fuzhou, China, in 2000, 2003, and 2010, respectively, where he is currently a Full Professor with the College of Mathematics and Computer Science. He also leads the Network Computing and Intelligent Information Processing Laboratory, which is a Key Laboratory of Fujian Province, China. His research interests include cloud computing, mobile computing, and evolutionary computation.